Growth and Characteristics of Near-UV LED Structures on Wet-etched Patterned Sapphire Substrate

Hung-Seob Cheong and Chang-Hee Hong

Abstract—**Patterned sapphire substrates (PSS) were fabricated by a simple wet etching process with SiO_2 stripe masks and a mixed solution of H_2SO_4 and H_3PO_4. GaN layers were epitaxially grown on the PSS under the optimized 2-step growth condition of metalorganic vapor deposition. During the 1st growth step, GaN layers with triangular cross sections were grown on the selected area of the surface of the PSS, and in the 2nd growth step, the GaN layers were laterally grown and coalesced with neighboring GaN layers. The density of threading dislocations on the surface of the coalesced GaN layer was 2~4 × 10^7 cm^{-2} over the entire region. The epitaxial structure of near-UV light emitting diode (LED) was grown over the GaN layers on the PSS. The internal quantum efficiency and the extraction efficiency of the LED structure grown on the PSS were remarkably increased when compared to the conventional LED structure grown on the flat sapphire substrate. The reduction in TD density and the decrease in the number of times of total internal reflections of the light flux are mainly attributed due to high level of scattering on the PSS.**

Index Terms—**Dislocation, GaN, Light emitting diodes, Metalorganic chemical vapor deposition, Patterned sapphire substrate, Wet etching**

Manuscript received May. 19, 2006; revised Aug. 3, 2006.
Semiconductor Physics Research Center/Department of Semiconductor Science and Technology, Chonbuk National University, Dukjin-dong, Dukjin-gu, Chonju, Chonbuk 561-756, Korea
E-mail : chhong@chonbuk.ac.kr

I. INTRODUCTION

Recently, near-UV light emitting diodes (LEDs) have attracted much interest as a strong candidate for the applications to solid-state lightings and high performance back light units in liquid-crystal displays. Those devices are still requiring a further improvement of the optical efficiency such as the internal quantum efficiency and the extraction efficiency. However, they strongly depend on the crystalline quality [1, 2] and the geometric shape of the LED dies [3], respectively. In the LED structures, the injected carriers can leak through defects [4, 5] and the light flux generated by the recombination of the carriers can be trapped in the LED dies due to their waveguide geometries of rectangular parallelepiped structures. In order to solve those problems, the growth techniques using dry-etched patterned sapphire substrates (PSS) have being used [6, 7]. In those techniques, however, a difficult dry etching process of sapphire substrates is required and a significant reduction of threading dislocations (TDs) is not reached as expected due to the relatively large area of vertical growth regions over the dry-etched PSS.

In this work, wet-etched PSS with V-grooves were used to grow GaN epitaxial layers, followed by the fabrication of LED structures with low TD density. The V-grooves on the wet-etched PSS were composed of sapphire crystal planes tilted from the horizontal c-plane of the substrate surface. The inclined crystal planes of the V-grooves provide the different growth rates to GaN epitaxial layers grown on the wet-etched PSS, which made possible to the lateral growth of GaN layer with low TD density. Both the low-defect density in the epitaxial layers and the substrate pattern contributed to increasing the optical performance of the fabricated LEDs.

II. EXPERIMENTAL PROCEDURE

The typical wet etching process to fabricate PSS, SiO_2 layer with thickness of 1000Å was deposited on sapphire substrate by plasma enhanced chemical vapor deposition and etched into SiO_2 stripe masks by the photolithography using the conventional wet etching method. The two different orientations <0-110>sapphire and <2-1-10>sapphire were chosen as the directions of SiO_2 stripe masks on the substrates. V-grooves were formed on the sapphire substrates by wet etching with a mixed solution of H_2SO_4 : H_3PO_4= 3 : 1. The etching temperature was between 270 ~ 280 C and the etch rate 1400 ~ 1800Å /min. The top width of the V-grooves was 5μm and that of the sapphire mesa between the grooves was 3μm. After the etching process, GaN epitaxial layers were grown on the wet-etched PSS by AIX200RF MOCVD system. Carrier gas was H_2, and trimethylgallium (TMGa) and ammonia (NH_3) were used as precursors for gallium and nitrogen, respectively. The GaN nucleation layer was deposited at the temperature of 560°C, the pressure of 400 mbar, and the V/III ratio of 2170. The high-temperature (HT) growth of GaN on the nucleation layer was performed by two growth steps for effective reduction of TDs over the entire region of the GaN layer. During the 1st growth step, GaN with a triangular cross-section grew from the sapphire mesa, and in the 2nd growth step, the GaN laterally grew over the V-grooves and coalesced into a flat layer. In the 1st growth step, the temperature and the pressure were 1020°C and 400 mbar, and in the 2nd growth step, the temperature and the pressure were 1140°C and 400 mbar, respectively. The V/III ratio was fixed at 1085 during both the two growth steps.

In order to verify the effect of TD density in the nitride epitaxial layers and the substrate pattern on the optical efficiency of LEDs, the near-UV LED structures (= 404 ~ 413 nm) with seven-period multi quantum wells (7MQWs) of InGaN (2.5nm)/GaN(11nm) pairs were grown on the two GaN layers on the PSS and the flat sapphire substrate in identical growth condition. First, 2-μm-thick n-GaN was grown on the GaN layers at 1120°C by using SiH_4 as a dopant source. The electron concentration of the n-GaN was 1.2×10^{19} cm^{-3}. After the growth of n-GaN, the MQWs were subsequently grown at 865C, and finally, a 110-nm-thick p-GaN with a hole concentration of 2.1×10^{17} cm^{-3} was grown at 1050°C by using biscyclopentadienyl magnesium (Cp2Mg) as a dopant source. Then, mesa-structure LEDs with 315 × 315 μm^2 area were fabricated by photolithography and dry etching by inductively coupled plasma. The Cr/Ni/Au and /Ni/Au layers were deposited by e-beam evaporation for contacts to the n- and p-type layers, respectively.

Etch profiles of the wet-etched PSS were observed by optical microscopy (OM). Density and propagation of TDswere observed by atomic force microscopy (AFM) and transmission electron microscopy (TEM), respectively. The crystalline quality and crystallographic tilt of GaN epitaxial layers was determined by X-ray rocking curves (XRCs) of (0002) and (10-12) reflections. The optical properties of the LEDs were characterized by photoluminescence (PL) and electroluminescence (EL). The current-voltage (I-V) measurements of the LEDs were performed using a parameter analyzer (HP 4156C).

III. RESULTS AND DISCUSSION

1. Low-defect GaN Layer on the Wet-etched PSS

Fig. 1(a) and (b) show the etch profile of the wet-etched PSS with V-grooves along the <1-100>sapphire and the <11-20>sapphire orientation, respectively. The etch profile depends on the direction of the V-groove. When the V-groove is parallel to the <1-100>sapphire orientation, the V-groove is symmetrical with respect to the <1-100>sapphire orientation and the inclined facets of the V-groove are near the {11-26} planes of the substrate. On the other hand, when the V-grooveis parallel to the <11-20>sapphire orientation, the V-groove is asymmetrical with respect to the <11-20>sapphire orientation and inclined facet is near the (-1102) r-plane and the other is near the (1-104) plane of the substrate. This symmetry is related to the r-plane symmetry of the α-sapphire crystal lattice shown in Fig. 1(c). The three grayed planes indicate the r-planes composing a triangular pyramid on the c-plane. Among the three r-planes, there are two r-planes symmetrical to each other with respect to the [1-100] orientation. This symmetry affect the etch profile of the V-groove along the [1-100]sapphire orientation as show in Fig. 1.(a). On

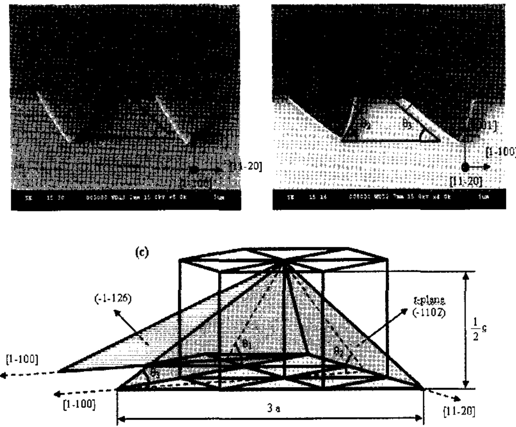

Fig. 1. Cross-sectional OM images showing etch profiles of the wet-etched PSS with V-grooves along (a) the <1-100>sapphire and (b) <11-20>sapphire orientations, respectively, and (c) a schematic diagram of the α-sapphire crystal lattice.

the other hand, the r-planes are not symmetrical to each other with respect to the [11-20] orientation, hence the etch profile of the V-groove along the [11-20]sapphire orientation is asymmetrical.

Fig. 2(a) - (d) show the cross-sectional OM images of GaN epitaxial layers grown on the PSS shown in Fig. 1(a) and (b). The high-temperature GaN growth succeeds the low-temperature nucleation, which was divided into two growth steps in order to reduce the TD density in both the vertical growth region on the sapphire mesa and the lateral growth region over the V-groove. The 1st growth step was to grow GaN layers with triangular cross-sections on sapphire mesas at the relatively low temperature of 1020 °C and the 2nd growth step was to grow the GaN layers in the lateral direction with a high lateral growth rate at the relatively high temperature of 1140°C. Comparing Fig. 2(a) and (b), the growth rate of the GaN layers grown on the inclined facets of the symmetrical V-grooves along the [1-100]sapphire orientation became increased during the 2nd growth step. Hence, the GaN layers grown in the symmetrical V-grooves blocked the lateral growth of the GaN layers grown on the symmetrical sapphire mesas during the 2nd growth step. On the other hand, the growth rate of the GaN layers grown on the inclined facets of the asymmetrical V-grooves along the [11-20]sapphire orientation was very low during both the 1st and the 2nd growth steps as shown Fig. 2(c) and (d). Thus, the GaN layers grown in the asymmetrical V-grooves did not block the lateral growth of the GaN layers grown on the

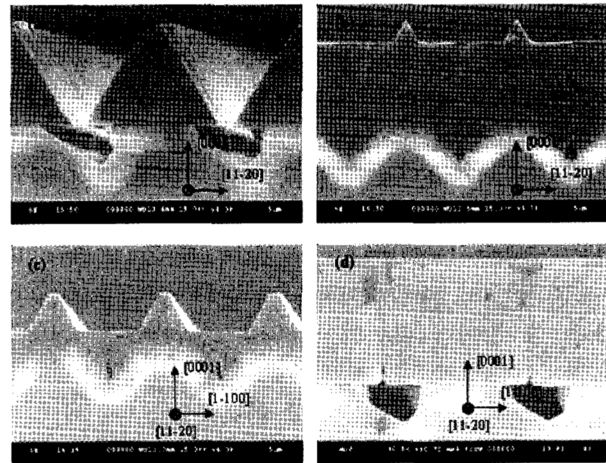

Fig. 2. Cross-sectional OM images of GaN epitaxial layer grown on the wet-etched PSS with V-grooves along (a), (b) the <1-100>sapphire and (c), (d) <11-20>sapphire orientations, respectively.

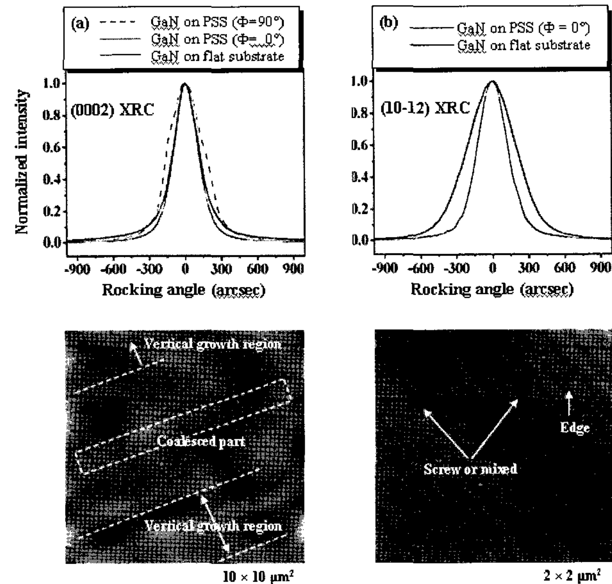

Fig. 3. (a) (0002) and (b) (10-12) XRCs for the conventional GaN layer on the FSS and for the GaN layer on the wet-etched PSS withV-grooves along the <11-20>sapphire orientation, and (c), (d) AFM images of the GaN layer on the wet-etched PSS.

asymmetrical sapphire mesas during the 2nd growth step. This result indicates that the PSS with asymmetrical V-grooves along the <11-20>sapphire orientation is much appropriate for the lateral growth of the low-defect GaN epitaxial layer.

Fig. 3(a) and (b) show XRCs of (0002) and (10-12) reflections for the GaN layers grown on the PSS with asymmetrical V-grooves and the conventional GaN layer grown on the flat sapphire substrate. The XRC is a good tool to characterize the mosaic structure of the GaN

layers grown on sapphire substrates [8, 9]. The mosaic structures of GaN layers can be characterized by tilt and twist angles. The tilt is the rotated angle of the GaN grains out of the (0002) growth plane and the twist is the rotated angle in the growth plane. The edge-type TDs with Burgers vector b = 1/3 <11-20> are resulted from the twist and distort all the planes except for the (0001) planes, and the screw-type TDs with Burgers vector b = <0001> are resulted from the tilt and distort all the planes except for the (hki0) planes, and the mixed-type TDs with Burgers vector b = 1/3<11-23> are divided into edge and screw dislocations and distort all the plane. Hence, the FWHM of the (0002) XRC is a figure of merit for the tilt and the density of TDs with a screw component, while that of the (10-12) XRC is a figure of merit for the tilt, the twist and the density of all TDs. As shown in Fig. 3(a), when the GaN layer grown the PSS is loaded for the V-grooves to be perpendicular (Φ = 90°) to the direction of X-ray beam, the (0002) XRC for the sample shows the FWHMs of 360 arcsec and the two shoulder peaks. The relatively broad FWHM and the shoulder peaks indicate that there is a crystallographic tilt between the GaN layers grown on the sapphire mesa and GaN wings suspending over the V-grooves. The GaN wing tilt is also observed in GaN layers grown by epitaxial lateral overgrowth or pendeo-epitaxy techniques [10]. The origin of the GaN wing tilt is due to the difference of strains between the GaN wings and the neighboringregions, which might be induced from the difference of a lattice mismatch, a thermal mismatch or other chemical and physical effects by mask materials on the two regions.

In order to compare the crystalline quality by XRC showing the minimized GaN wing tilt, the GaN sample grown on the PSS is loaded for the V-grooves to be parallel (Φ = 0°) to the direction of X-ray beam. The FWHM of (0002) XRC for GaN layer grown on the PSS is 234 arcsec, which is a little narrower than 252 arcsec for the conventional GaN layer grown on the flat sapphire substrate as shown in Fig. 3(a). This result indicates that the reduction of TDs with a screw component is relatively small by the lateral growth technique in this study. However, the FWHM of (10-12) XRC for GaN layer grown on the PSS is 306 arcsec, which is a much narrower than 468 arcsec for the conventional GaN layer as shown in Fig 3(b). The comparison of the FWHMs of (0002) and (10-12) XRCs is indicative of the drastic reduction of edge-type TDs by using the PSS.

The reduction of TDs was confirmed by the AFM images of the GaN layer grown on the PSS shown in Fig. 3(c) and (d). Since AFM image is not sensitive to the edge-type TDs on the as-grown surface of the GaN layer, the GaN surface was etched in a mixed solution of H_2SO_4 and H_3PO_4 (H_2SO_4 : H_3PO_4 = 3 : 1) at 200°C for 10 minutes in order to observe the etch pits corresponding to all the types of TDs. As shown in Fig. 3(c), the TD densities of both the vertical and the lateral growth regions are lower than that of the conventional GaN layer grown on the flat sapphire substrate showing the TD density about ~ 10^{10} cm^{-2}. From repeated measurement of AFM, the etch-pit density was about 2 ~ 4 × 10^7 cm^{-2} for the GaN layer grown on the PSS. The etch pits observed by AFM images can be divided into two categories [11, 12]. As shown in Fig 3(d), the small etch pits are located in the terraces and the large etch pits are located at the origins of atomic steps. The edge-type TDs whose Burgers vectors do not have a c-direction component correspond to the small etch pits in the terraces, and screw- or mixed-type TDs whose Burgers vectors have a c-direction component correspond to the large etch pits associated with the step terminations. Based on the AFM images, the edge-type TDs are about 32 % and the rest about 68 % are screw- or mixed-type TDs, which is different from the TD density of the conventional GaN grown on the flat sapphire substrate predominantly showing edge-type TDs. This result indicate that the density of edge-type TDs is drastically reduced and the reduction of the density of screw- or mixed-type TDs is not so much due to the newly appeared TDs at the tilted boundary of GaN wings as shown in Fig. 3(c). This result agree well with the XRC results for GaN layer grown on the PSS showing the small reduction of the FWHM of (0002) XRC and the large reduction of the FWHM of (10-12) XRC, when compared to the conventional GaN layer.

Fig. 4(a) and (b) show cross-sectional TEM images of a vertical growth region of the GaN layer grown on the PSS with the asymmetrical V-grooves. As shown in Fig. 4(a), the TDs near the edge of the sapphire mesa are bent to horizontal directions. This bending phenomenon of TDs is occurred on the inclined {11-22} facets of the

GaN layer formed during the 1st growth step. Thus, the formation of triangular cross-sections of the GaN layers during the 1st growth step is effective for the reduction of TDs in the vertical growth region on the sapphire mesa. This observation was confirmed by the TEM image of the vertical growth region near the surface shown in Fig. 4(b). It is difficult to observe TDs near the surface of the vertical growth region as shown in the image. These results agree well with the AFM image shown in Fig. 3(c) and indicate that the TD density can be effectively reduced in the vertical growth region as well as in the lateral growth region by the 2-step growth condition in this study.

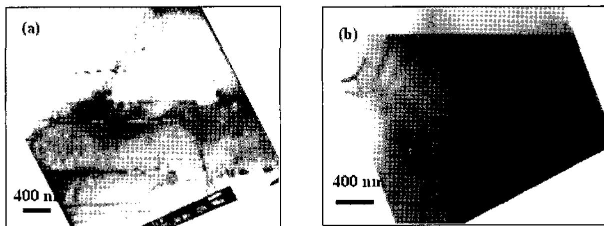

Fig. 4. Cross-sectional TEM images of a vertical growth region of the GaN layer on the wet-etched PSS with V-grooves along the <11-20>sapphire orientation: (a) shows the region near the GaN/sapphire interface and (b) shows the region beneath the free surface.

2. Low-defect LED Structures on the Wet-etched PSS

The surface AFM images of the GaN layers grown on the FSS and the wet-etched PSS with asymmetrical V-grooves are shown in Fig. 5 (a) and (b), respectively, which confirm the significant reduction in TD density of the GaN template grown on the wet-etched PSS. Both the GaN templates were used to grow the near-UV LED structures on them. Fig. 6 shows the TEM images of the two MQW structures grown on GaN template on the

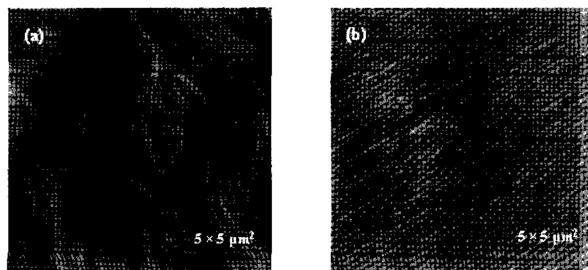

Fig. 5. AFM images of the GaN layers grown on (a) the FSS and (d) the wet-etched PSS.

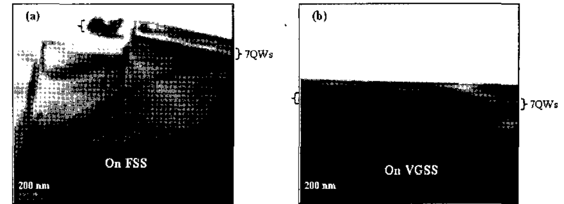

Fig. 6. Cross-sectional TEM images of the MQW structures over (a) the FSS and (b) the wet-etched PSS.

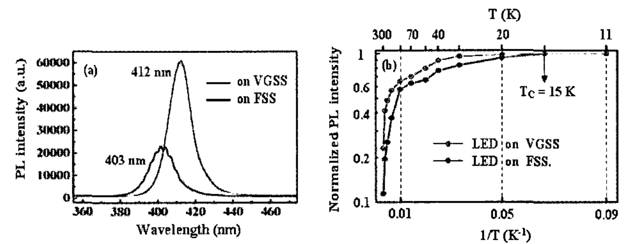

Fig. 7. (a) RT-PL spectra and (b) normalized PL intensities versus the inverse temperatures of the LED structures on the FSS and the wet-etched PSS.

wet-etched PSS and the conventional GaN template on the FSS. Based on the TEM images, the TD density was found to be much lower in the MQWs grown on the VGSS. Additionally, from high-resolution TEM images and $\omega/2\theta$ scans of x-ray diffraction, the periods of MQWs of the two samples are the same, but the interfaces of the MQWs grown on the PSS was more abrupt. The better crystalline quality of the MQWs on the PSS is expected to contribute to the increase of the internal quantum efficiency (η_{int}) of the LED structure on it.

Fig. 7 (a) and (b) show the results of PL measurements for the two LED samples. As shown in the room-temperature PL spectra of Fig. 7 (a), the peak from MQWs over the wet-etched PSS is red- shifted by 9 nm with respect to the MQWs over the FSS. This observation indicates that the In incorporation is in higher level in the MQWs over the VGSS. Fig. 7 (b) shows the normalized PL intensities measured at low temperatures ranging from 11 K to 300 K. The PL intensity is strongest at 15 K and is almost constant at the lower temperature. Thus, the critical temperature T_c indicating the saturation point of the intensities is 15 K. The internal quantum efficiency of the two LED samples can be estimated by the assumption that there is no non-radiative recombination process at the critical temperature. The internal quantum efficiency η_{int} can be written as η_{int} (%) = $I(T)/I(T_c)$ 100, where I(T) is the PL intensity at the temperature T, and $I(T_c)$ is the PL

intensity at the critical temperature Tc [13]. By using this equation, the η_{int} of the LED on the FSS is calculated as 11%, and the η_{int} of the LED on the wet-etched PSS is 23%. As for the extraction efficiency of the two LED samples simulated by the commercial Light Tool program, the extraction efficiency of the LED structure on the PSS was higher by a factor of 1.3 than that of the same LED structure on the FSS.

Fig. 8 (a) shows the logarithmic I-V curves of the two mesa-structure LEDs on the wafer. Under the reverse bias of -10 V, the leakage current due to the generation of carriers in trap levels is 0.2μA in the LED on the wet-etched PSS, which is far less than 2.9μA of the LED on the FSS. In the low forward bias regime below 2V, the non-radiative recombination current through trap levels is less in the LED on the PSS. These results indicate that the density of defects acting as trap levels is lower in the LED on the PSS. Fig. 8 (b) shows the optical output power by the electrical driving of the two LED samples. The output power of the LED on the wet-etched PSS is higher than that of the LED on the FSS by a factor of 2.6. This result agrees well with the previous data showing the higher internal quantum efficiency and the higher extraction efficiency of the LED structure on the wet-etched PSS.

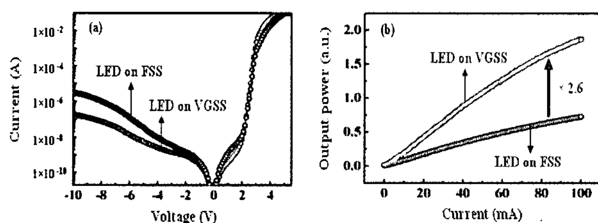

Fig. 8. (a) Logarithmic I-V curves and (b) the optical output power versus the dc forward current of the LEDs on the FSS and the wet-etched PSS.

IV. SUMMARY

Two types of PSS with different orientations of V-grooves were fabricated by a simple wet etching process with a mixed solution of H_2SO_4 and H_3PO_4. The low-defect GaN epitaxial layers were successfully grown on the wet-etched PSS with the asymmetrical V-grooves along the <11-20>sapphire orientation under the optimized 2-step growth condition. By the 2-step growth condition, the TD density was significantly reduced in the vertical growth region as well as in the lateral growth region. The reduction of TDs were mainly pronounced by the edge-type TDs as demonstrated from the results of XRCs and AFM images. The density of all TDs on the surface of the GaN layer grown on the wet-etched PSS was about 2 ~ 4 × 10^7 cm^{-2}. The internal quantum efficiency of the LED on the wet-etched PSS was about two times higher than that of the LED on the FSS. With the contribution of the increased extraction efficiency, the output power of the LED on the VGSS was higher by a factor of 2.6 than that of the LED on the FSS.

ACKNOWLEDGMENTS

This work was supported by grant No. R01-2004-000-10390-0 from the Basic Research Program of the Korea Science & Engineering Foundation

REFERENCES

[1] S. Watanabe et al., "Internal quantum efficiency of highly-efficient InxGa1–xN-based near-ultraviolet light-emitting diodes," *Appl. Phys. Lett.*, 83, p.4906, 2003.

[2] Y. H. Cho et al., "Carrier loss and luminescence degradation in green-light-emitting InGaN quantum wells with micron-scale indium clusters," *Appl. Phys. Lett.*, 83, p.2578, 2003.

[3] T. Fujii, Y. Gao, R. Sharma, E. L. Hu, S. P. DenBaars, and S. Nakamura, "Increase in the extraction efficiency of GaN-based light-emitting diodes via surface roughening," *Appl. Phys. Lett.*, 84, p. 855, 2004.

[4] E. G. Brazel, V. Narayanamurti, and M. A. Chin, "Direct observation of localized high current densities in GaN films," *Appl. Phys. Lett.*, 74, p. 2367, 1999.

[5] C. Y. Hsu, W. H. Lan, and Y. S. Wu, "Effect of thermal annealing of Ni/Au ohmic contact on the leakage current of GaN based light emitting diodes," *Appl. Phys. Lett.*, 83, p. 2447. 2003

[6] M.Yamada, T. Mitani, Y. Narukawa, S. Shioji, I.

Niki, S. Sonobe, K. Deguchi, M. Sano, and T. Mukai, "InGaN-Based Near-Ultraviolet and Blue-Light-Emitting Diodes with High External Quantum Efficiency Using a Patterned Sapphire Substrate and a Mesh Electrode ," *Jpn. J. Appl. Phys.*, 41, p. 1431, 2002.

[7] K. Tadatomo, H. Okagawa, Y. Ohuchi, T. Tsunekawa, T. Jyouichi, Y. Imada, M. Kato, H. Kudo, and T. Taguchi, "High Output Power InGaN Ultraviolet Light-Emitting Diodes Fabricated on Patterned Substrates Using Metalorganic Vapor Phase Epitaxy," *phys. stat. sol. (a)*, 188, p. 121, 2001.

[8] B. Heying, X. H. Wu, S. Keller, Y. Li, D. Kapolnek, B. P. Keller, S. P. DenBaars, and J. S. Speck, "Role of threading dislocation structure on the x-ray diffraction peak widths in epitaxial GaN films ," *Appl. Phys. Lett.*, 68, p. 643, 1996.

[9] Y. B. Pan, Z. J. Yang, Z. T. Chen, Y. Lu, T. J. Yu, X. D. Hu, K. Xu, and G. Y. Zhang, "Reduction of threading edge dislocation density in n-type GaN by Si delta-doping," *J. Crystal Growth*, 286, p. 255, 2006.

[10] H. S. Cheong, Y. K. Hong, C.-H. Hong, Y. H. Choi, S. J. Leem, and H. J. Lee, "Improvement of Structural Properties of GaN Pendeo-Epitaxial Layers," *phys. stat. sol. (a)*, 192, p. 377, 2002.

[11] H. P. D. Schenk, P. Venngus, O. Tottereau, T. Riemann, and J. Christen, "Three-dimensionally nucleated growth of gallium nitride by low-pressure metalorganic vapour phase epitaxy," *J. Crystal Growth*, 258, p. 232, 2003.

[12] J. Bai, T. Wang, P. J. Parbrook, K. B. Lee, and A.G. Cullis, "A study of dislocations in AlN and GaN films grown on sapphire substrates," *J. Crystal Growth*, 282, p. 290, 2005.

[13] Y. Kawakami et. al., "Radiative and Nonradiative Recombination Processes in GaN-Based Semiconductor," *phys. stat. sol. (a)*, 183, p. 41, 2001.

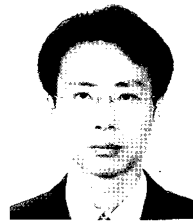

Hung-Seob Cheong was born in Imsil-gun in Jeollabuk-do, Korea in 1975. He has received his master's degree in Semiconductor Science and Technology from Chonbuk National University (CBNU), Jeollabuk-do, Korea in February 2003. He had completed the doctoral course of study in the department of Semiconductor Science and Technology of CBNU in August 2004 and is presently working as a Ph. D. candidate in the same department of CBNU. He has published more than 15 research papers in international journals and conference proceedings. His present research interests include growth, fabrication and characterization of high-performance III-nitride optical devices.

Chang-Hee Hong was born in Seoul, Korea in 1956. He received the B. E. degree in the department of Electronic Engineering from Korea University, in 1984; M.S. degree and Ph. D. degree in the department of Electrical and Electronics Engineering from Korea Advanced Institute of Science Technology, Seoul, Korea in 1986 and 1991, respectively. From 1991 to 1994, he has worked as Research fellow in the Department of Electronics and Electrical Engineering of the University of Michigan, Ann Arbor, U.S.A. He has worked as Principal Researcher at OE group of LG Cooperated Institute of Technology from 1994 to 1998. Now he is an Associate Professor in the Department of Semiconductor Science and Technology and Semiconductor Physics Research Center, Chonbuk National University, Jeonju, Korea since 1998. He has published more than 100 research papers in international journals and conference proceedings. His present research interests include MOCVD growth and characterization of GaN based epitaxial layers, fabrication of high performance white and green GaN LED, thermal characterization of high power LED, and novel quantum wire based optoelectronic devices.